Internal rotation effects in the rotationally resolved $S_1(^1L_b) \leftarrow S_0$ origin bands of 3-methylindole and 5-methylindole

Karen Remmers, Erko Jalviste, Ivan Mistrík, Giel Berden, and W. Leo Meerts
Department of Molecular and Laser Physics, University of Nijmegen, Toernooiveld, 6525 ED Nijmegen, The Netherlands
Institute of Physics, Tartu University, Riia 142, EE2400 Tartu, Estonia

The rotationally resolved UV excitation spectra of the $S_1(^1L_b) \leftarrow S_0$ origin bands of 3-methylindole and 5-methylindole have been measured and analyzed. As a result of an internal rotation of the methyl group, each spectrum consists of rotational lines of overlapping $0a_1 \leftarrow 0a_1$ and $0e \leftarrow 0e$ torsional transitions. Like indole, 3-methylindole and 5-methylindole undergo axis reorientation upon electronic excitation. The Hamiltonian used to describe all observed spectral features includes a pure rotational part, a pure torsional part, and terms describing the interaction between the internal rotation and the overall rotation. It also accounts for the axis reorientation effect. Values for the barrier heights of the methyl torsion, the angle of the methyl top axis with the inertial axes, and the rotational constants are obtained for both the S_0 and the S_1 state. From an analysis of the intensities of the rotational transitions, the direction of the transition moment and the axis reorientation angle are obtained. Due to quantum interference effects in the 5-methylindole spectrum the sign of these angles could be determined.

I. INTRODUCTION

Indole, its derivatives and complexes have attracted significant attention because indole is a chromophore of the amino acid tryptophan. In these molecules the π-conjugated electrons give rise to two close lying electronically excited states, labeled ^1L_a and ^1L_b. Excitation to the ^1L_a state causes a significantly larger amount of charge transfer than does excitation to the ^1L_b state.[1,2] This larger charge transfer is responsible for the much larger solvent and substitution shifts for $^1L_a \leftarrow S_0$ transitions in comparison with $^1L_b \leftarrow S_0$ transitions.[1,3]

Methyl substitution into different sites can provide a spectroscopic probe of the electronic structure of the parent molecule since the methyl torsional barrier height is sensitive to the π electron density of the bonds adjacent to the methyl group.[4–6] Following this line of thought Bickel *et al.*[7] analyzed the torsional excitation and dispersed fluorescence spectra of the $S_0 - S_1$ transitions of seven monomethyl indoles. For 5-methylindole and 6-methylindole a long torsional progression was observed, which was explained by a phase shift between the S_0 and S_1 torsional potentials owing to the 60° rotation of the methyl group upon excitation. No phase shift was found for the other methylindoles. For 2-methylindole and 3-methylindole (skatole) only the origin band was observed due to the lack of Franck-Condon activity; it was not possible to determine the barrier heights. Later, Sammeth *et al.*[8] presented a vibrational and rotational band contour analysis of 3-methylindole (3-MI) and 5-methylindole (5-MI) by using one- and two-photon laser induced fluorescence spectroscopy. For 3-MI it was possible to assign two of the weak bands near the origin to the transitions terminating in the $2a_1$ and $2e$ torsional levels of S_1.[9]

Another point of interest is the possibility of 'tuning' the frequency spacing between ^1L_a and ^1L_b states, which depends on the site to which the methyl group is attached and on the solvent that is used.[10,11] The ^1L_a–^1L_b spacing will influence the frequencies and intensities of the whole excitation spectrum due to the vibronic interactions between the two states. It has been shown that in solutions the electronically excited states are widely separated for 5-MI but approach each other for 3-MI.[12] Several studies were performed in order to distinguish between the two different electronic states and determine the position of the ^1L_a origin of different indole derivatives.[10,13–17] Polarized two-photon excitation spectroscopy enabled Sammeth *et al.*[15] to discriminate between ^1L_a and ^1L_b type bands of jet-cooled 3-MI and 3-trideuteromethylindole. A number of intense ^1L_a type vibronic bands were identified in this way. Albinsson *et al.*[18] determined the transition moment directions for both ^1L_a and ^1L_b states of indole, 3-MI, 5-MI and 5-methoxyindole oriented in stretched polyethylene films, and showed that the transition moments of ^1L_a and ^1L_b were almost perpendicular to each other.

Rotationally resolved spectra of molecules with an internal rotation degree of freedom can provide several important molecular properties (the rotational constants for the ground and excited state, the direction of the methyl top axis and the transition moment angle) that cannot be determined precisely by other techniques.[19–21] Besides this, a joint analysis of rotational and torsional data can yield more accurate values for torsional barrier heights. In both 3-MI and 5-MI the interaction between torsion and overall rotation of the molecule perturbs the rotational spectra. For these molecules a vibration-torsion analysis is already performed,[8,15] a prerequisite for the high resolution measurements. In this paper, we present the full (frequency and intensity) analysis of rotationally resolved fluorescence excitation spectra of the origin bands of the $S_1(^1L_b) \leftarrow S_0$ transitions of 3-MI and 5-MI.

II. THEORY

A. Model and Calculations

The choice of an appropriate model for analyzing the measured spectra is important for the extraction of a maximum amount of information (molecular constants and their error limits) within a reasonable computing time. Both 3-MI and 5-MI are assumed to consist of a methyl top attached to a planar frame (indole). The methyl top axis and the transition dipole moment are assumed to lie in the plane of the indole frame in both the ground and excited state. Molecules of this type belong to the molecular symmetry group G_6, which has three symmetry species, a_1, a_2, and e.[22,23] We consider only one large amplitude motion, which is the methyl top torsion (internal rotation) around its symmetry axis. In our calculations the reference coordinate system is formed by the principal inertial axes (the principal axis method, PAM). In this method the rotational constants are directly related to the geometry of the entire molecule and do not include contributions from internal rotation.

In general, the solution of the torsion-rotation problem can be described by the Hamiltonian:[24,25]

$$H_{tr} = F(p - \boldsymbol{\rho} \cdot \boldsymbol{J})^2 + V(\alpha) + AJ_a^2 + BJ_b^2 + CJ_c^2 \tag{1}$$

in a torsion-rotation basis $|e^{im\alpha}\rangle|J, K\rangle$. Here, F is the internal rotation constant:

$$F = \hbar^2/2rI_\alpha = F_\alpha/r, \tag{2}$$

where

$$r = 1 - I_\alpha \sum_g \cos^2 \eta_g / I_g, \tag{3}$$

$p = -i\hbar\frac{\partial}{\partial\alpha}$ is the angular momentum operator conjugate to the torsional angle α, $V(\alpha)$ is the torsional potential function, A, B, C are the rotational constants, and J_a, J_b, J_c are the projections of the total angular momentum on the principal inertial axes a, b, and c of the molecule. The components of the vector $\boldsymbol{\rho}$ are given by the direction cosines $\cos\eta_g$ of the methyl top axis in the principal axis system, the moments of inertia of the entire molecule I_g ($g = a, b, c$), and the moment of inertia of the methyl group I_α:

$$\rho_g = \cos\eta_g I_\alpha / I_g. \tag{4}$$

For the methylindoles $\rho_c = 0$, since the methyl top axis lies in the ab plane; we write $\cos\eta_a = \cos\eta$ and $\cos\eta_b = \sin\eta$, where η is the methyl top angle with respect to the a-axis (left part of Fig. 1).

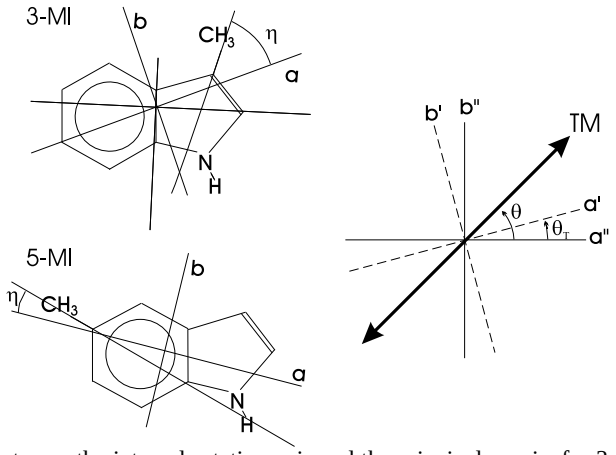

FIG. 1. Definition of η, the angle between the internal rotation axis and the principal a axis, for 3-methylindole and 5-methylindole (left panel). In the right panel the transition moment angle θ and the axis reorientation angle θ_T are defined. Angles measured in counterclockwise sense are taken to be positive. a'' and b'' are the principal axes in the ground state, a' and b' are the principal axes in the excited state. The c axes are perpendicular to the indole frame.

An exact solution of Eq. (1) is impractical for spectra containing lines starting from high J levels, because of the long computational time needed. We therefore applied a perturbation approach,[19,24,25] which permits us to solve the torsion and rotation problems separately. First, the pure torsional Hamiltonian is solved. The torsional Hamiltonian is expressed as:[22,24]

$$H_t = Fp^2 + V_3(1-\cos 3\alpha)/2 + V_6(1-\cos 6\alpha)/2. \tag{5}$$

Eigenfunctions of this Hamiltonian are given by:

$$|\nu\sigma\rangle = \sum_{k=-\infty}^{\infty} A_k^{(\nu)} e^{i(3k+\sigma)\alpha}, \tag{6}$$

where ν is the torsional level label and σ can take on the values -1, 0 and $+1$.[22,24] This label indicates the symmetry of the torsional functions; levels with $\sigma = 0$ are of a symmetry and levels with $\sigma = \pm 1$ (two-fold degenerate levels) are of e symmetry.

Treating the interaction of the torsion with the overall rotation as a perturbation in the rotational Hamiltonian, an effective rotational Hamiltonian can be constructed for each $\nu\sigma$ torsional level:[24,25]

$$H_{\nu\sigma} = AJ_a^2 + BJ_b^2 + CJ_c^2 + F\sum_{n=1}^{\infty} W_{\nu\sigma}^{(n)} (J_a\rho_a + J_b\rho_b)^n, \tag{7}$$

where $W_{\nu\sigma}^{(n)}$ is the n-th order perturbation coefficient for the $\nu\sigma$ level. The dimensionless perturbation coefficients $W_{\nu\sigma}^{(1)}$ and $W_{\nu\sigma}^{(2)}$ can be expressed in terms of matrix elements of the internal rotation angular momentum operator p in the basis of the torsional wave functions given in Eq. (6):[24]

$$\begin{aligned} W_{\nu\sigma}^{(1)} &= -2\langle \nu\sigma|p|\nu\sigma\rangle \\ W_{\nu\sigma}^{(2)} &= 1 + 4F\sum_{(\nu\sigma)'}{}' \frac{|\langle \nu\sigma|p|(\nu\sigma)'\rangle|^2}{E_{\nu\sigma} - E_{(\nu\sigma)'}}, \end{aligned} \tag{8}$$

where $E_{\nu\sigma}$ and $E_{(\nu\sigma)'}$ are the torsional energies of the $\nu\sigma$ and $(\nu\sigma)'$ levels. Higher order coefficients $W_{\nu\sigma}^{(n)}$ can be expressed in terms of $W_{\nu\sigma}^{(1)}$ and $W_{\nu\sigma}^{(2)}$ *via* the relationship:[24,25]

$$\frac{W_{\nu\sigma}^{(n+2)}}{W_{\nu\sigma}^{(n)}} \approx \frac{-(2\pi/3)^2}{(n+1)(n+2)} \quad \text{for } n > 0. \tag{9}$$

For the non-degenerate states (a levels), all odd-order perturbation terms are zero.[24,25] This implies that for these states the rotational Hamiltonian in first approximation is given by a rigid rotor Hamiltonian with effective rotational constants:[24]

$$\begin{aligned} A_{\nu\sigma} &= A + FW_{\nu\sigma}^{(2)}\rho_a^2 \\ B_{\nu\sigma} &= B + FW_{\nu\sigma}^{(2)}\rho_b^2 \\ C_{\nu\sigma} &= C + FW_{\nu\sigma}^{(2)}\rho_c^2. \end{aligned} \tag{10}$$

For e levels also the odd-order perturbation terms should be taken into account. In both cases rotational basis functions up to $\Delta K = 4$ are mixed by the matrix elements for the effective rotational Hamiltonian [Eq. (7)] up to 4th order, which are given in Appendix B of Ref. 25.[26] The matrix of size $(2J+1)\times(2J+1)$ was diagonalized for every J for the two lowest torsional states, $0a_1$ and $0e$. K_a and K_c labels were assigned to the calculated rotational levels of a given J by their energy ordering, despite of the absence of a clear physical meaning of K_a (and especially K_c) labels in the presence of the torsion-rotation interaction.[23] The intensities of the rotational lines are calculated from the eigenvectors of the effective rotational Hamiltonian and the known direction cosine matrix elements.[24] The only selection rule used is $\Delta J = 0, \pm 1$ which distinguishes P, Q, and R branches. If the transition dipole moment (TM) vector lies in the ab plane the line strength is proportional to:

$$A_{r''r'} \propto |\mu_a\langle r'|\Phi_{Za}|r''\rangle|^2 + |\mu_b\langle r'|\Phi_{Zb}|r''\rangle|^2 + 2\mu_a\mu_b\langle r'|\Phi_{Za}|r''\rangle\langle r'|\Phi_{Zb}|r''\rangle, \tag{11}$$

where the Z-axis is the space-fixed axis along the direction of the laser polarization, $|r\rangle \equiv |J, K_a, K_c\rangle$, $\mu_a = \mu\cos\theta$, and $\mu_b = \mu\sin\theta$. The double and single prime denote the ground and excited state, respectively, μ is the absolute value of the transition dipole moment (TM), θ is the angle of the TM vector with respect to the molecule-fixed a-axis, and Φ_{Za} and Φ_{Zb} are the direction cosines between the laboratory Z-axis and the molecular a- and b-axes.

Indole, the chromophore of 3-MI and 5-MI, shows axis reorientation upon electronic excitation.[27] The principal axis system rotates around the c-axis (see Fig. 1) and although the angle of rotation is small, only 0.5°, the effect on the intensities of the

rotational transitions is very pronounced. For a correct calculation of the intensities all rotational wave functions of the ground and the excited state should be expressed in a common coordinate system. This can be achieved by transforming the excited state Hamiltonian *via* a rotation of **J** around the *c*-axis by an angle θ_T:[27,28]

$$\begin{aligned} H^t_{\nu'\sigma'} &= (A'\cos^2\theta_T + B'\sin^2\theta_T)J_a'^2 + (A'\sin^2\theta_T + B'\cos^2\theta_T)J_b'^2 + C'J_c'^2 \\ &\quad +(A'-B')\sin\theta_T\cos\theta_T(J_a'J_b' + J_b'J_a') \\ &\quad +F'\sum_{n=1}^{\infty} W^{(n)}_{\nu'\sigma'}[(\rho_a'\cos\theta_T - \rho_b'\sin\theta_T)J_a' + (\rho_a'\sin\theta_T + \rho_b'\cos\theta_T)J_b']^n. \end{aligned} \tag{12}$$

In this way the excited state Hamiltonian is expressed in the coordinate system of the ground state and its eigenfunctions can therefore be given within the same basis set as the ground state functions.[29] It is readily seen that the matrix elements of the transformed effective rotational Hamiltonian [Eq. (12)] are the same as those for the effective rotational Hamiltonian [Eq. (7)], with the exception that the constants A, B and C and ρ_a and ρ_b are replaced by variables depending on the transformation angle θ_T. The cross term $J_aJ_b + J_bJ_a$ however, gives rise to a new matrix element

$$\langle JK|(J_aJ_b + J_bJ_a)|JK\pm1\rangle = \frac{1}{2}(2K\pm1)[J(J+1) - K(K\pm1)]^{\frac{1}{2}}. \tag{13}$$

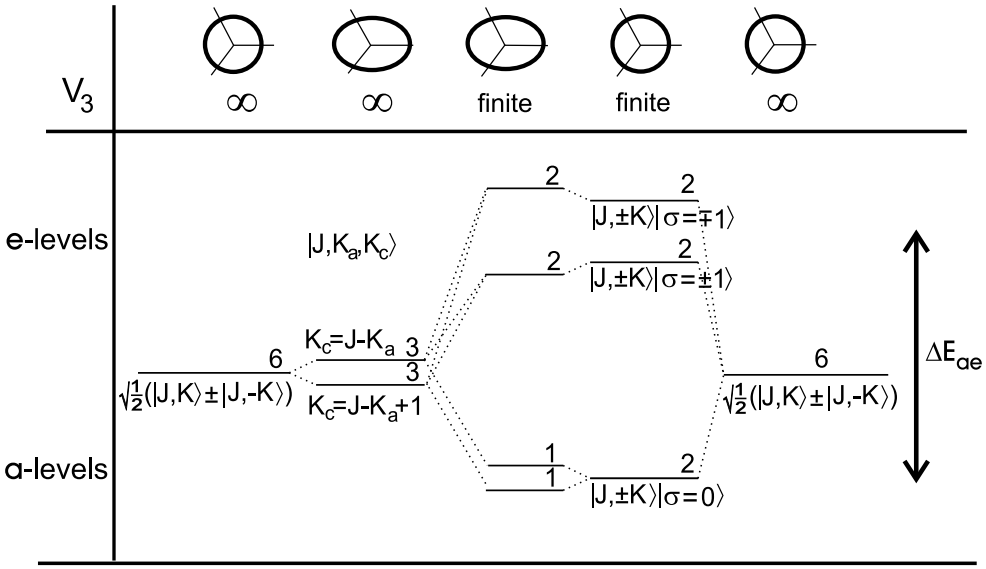

FIG. 2. Correlation diagram, showing the effects of internal rotation on the energy and characterization of symmetric and asymmetric rotor levels. The figures on top of the diagram represent the symmetry of the rotor, while directly below the barrier height indicates whether there is internal rotation (finite barrier) or not (infinite barrier). The degeneracy of the levels is given by the numbers above each level. Where possible a characterization of each level is given. ΔE_{ae} equals the torsional level splitting.

B. Effects on rotational spectra

The most apparent effect of the internal motion of the methyl group on the rotational spectra of the $S_1 \leftarrow S_0$ origin bands is the occurrence of two overlapping spectra arising from transitions between levels with different torsional symmetries ($0a_1-0a_1$ and $0e-0e$ transitions). The two spectra can each be described by an effective rotational Hamiltonian, which accounts for the interaction between torsion and overall rotation [Eq. (7)]. The two origins will be shifted by:

$$\Delta\nu_0^{ae} = \Delta E'_{ae} - \Delta E''_{ae}, \tag{14}$$

where $\Delta E''_{ae}$ and $\Delta E'_{ae}$ are the torsional splittings between the $0a_1$ and $0e$ levels in the ground and excited state, respectively. The torsional level splitting is larger for lower barriers; hence, a lowering of the barrier upon excitation will cause a blue shift of the $0e-0e$ origin with respect to the $0a_1-0a_1$ origin.

Since all the odd perturbation coefficients vanish for *a* levels, the effects of the internal rotation interaction are largest for the *e* levels. For these levels the rigid rotor wavefunctions are mixed. The mixing due to odd powers of J_a increases with increasing values of K_a and the mixing due to odd powers of J_b decreases with increasing values of K_a. Fig. 2 schematically shows the effects

of both asymmetry and internal rotation on the rigid symmetric rotor levels and displays the correlation of perturbed asymmetric rotor levels with rigid asymmetric rotor levels on the one hand and perturbed symmetric rotor levels on the other hand.

The mixing of K_c values causes a splitting of (almost) degenerate K doublets and the appearance of lines that are forbidden in the asymmetric rigid rotor limit, as illustrated in Fig. 3. This is especially apparent in transitions involving high K_a levels of the 0*e* state, where the mixing of K_c values can be almost complete. The stronger the mixing of wavefunctions the more intense the 'forbidden' lines will be. For low K_a values there will be two strong rigid rotor allowed and two weak anomalous lines. For high K_a values there will be two weak 'allowed' and two strong anomalous lines. For some intermediate K_a value there will be four lines of comparable intensity.

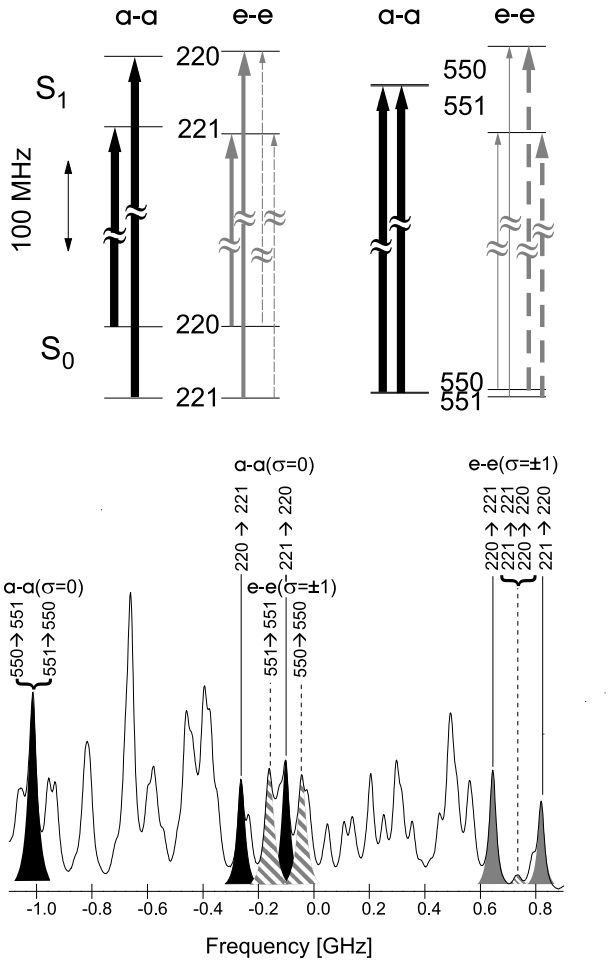

FIG. 3. Effect of internal rotation on *a*-type transitions in the Q-branch of 3-methylindole. Upper panel: e levels with high J, K_a value are split by $FW_{0e}^{(1)}\rho_a K_a$. The width of the arrows corresponds (approximately) to the strength of the transitions; the 0e–0e transitions show a change from 'normally allowed' transitions ($\Delta K_c = \pm 1$) for low K_a values, where the asymmetry splitting is large, to anomalous transitions ($\Delta K_c = 0$) for high K_a values, where the asymmetry splitting is much smaller. This is also illustrated by part of the experimental spectrum of 3-methylindole (lower panel), where the corresponding transitions are marked.

Because rigid rotor wavefunctions of different K_a parity are mixed, as well, the line strength of a transition is no longer described by only one term in Eq. (11). A transition can be induced by both the *a* and *b* component of the TM (such a transition is no longer a pure *a* or pure *b* type transition). The interference term in the line strength formula [Eq. (11)] makes it possible to distinguish positive and negative angles of the TM, as first discussed by Plusquellic *et al.*[30] A change of the sign of this angle would change the sign of the interference term and therefore affects the intensities.

Axis reorientation also mixes the wavefunctions, as can be seen from Eq. (12). The term proportional to $(J_a J_b + J_b J_a)$ couples states with different K_a parities and therefore mixes the character of *a* and *b* type lines.[28] Unlike the internal rotation induced mixing, axis reorientation affects *a* and *e* symmetry levels in a similar way.

C. Computational Approach

All assigned rotational lines in the overlapping $0a_1-0a_1$ and $0e-0e$ spectra were fit simultaneously with torsional frequencies from the literature if available. There are several advantages to this approach in comparison with the separate analysis of the $0a_1-0a_1$ and $0e-0e$ spectra. (i) The perturbation coefficients and the torsional barrier heights are more accurate, since the vibrational band frequencies and rotational line frequencies are used in a self-consistent way. (ii) An important structural parameter, the angle of the methyl top axis is obtained directly from the fit. (iii) The 'torsion-free' rotational constants, which are directly related to the corresponding moments of inertia of the molecule, are immediately obtained. (iv) The assignment of extensively overlapping lines is much easier if the measured spectrum is directly compared with the composite $0a_1-0a_1/0e-0e$ spectrum.

We start by fitting the frequencies of the rotational lines and torsional transitions to the torsional and effective rotational Hamiltonians [Eqs. (5) and (7)]. A maximum of 15 parameters can be determined, including the rotational constants A, B and C of the ground and electronically excited states, the torsional barrier heights in both states and the frequency of the $0a_1-0a_1$ band origin.

The constants resulting from the frequency fit are kept fixed in the intensity fit, where 10 additional parameters can be determined; the rotational population distribution parameters T_1, T_2, and w (see below), the transition dipole moment angle θ, the axis reorientation angle θ_T, the intensity ratio of the $0e-0e$ and $0a_1-0a_1$ spectra I_e/I_a, the Lorentzian and the Gaussian contributions to the width of the Voigt-shaped lines, the background intensity and an intensity scaling factor. The importance of these parameters has been extensively discussed in Ref. 27.

The intensity ratio of the $0e-0e$ and $0a_1-0a_1$ spectra is given by:

$$\frac{I_e}{I_a} = \frac{g_e \cdot n_{Se} \cdot S_e \cdot n_e}{g_a \cdot n_{Sa} \cdot S_a \cdot n_a}, \tag{15}$$

where g_e and g_a are the degeneracies of the $0a_1$ and $0e$ levels ($g_e = 2$ and $g_a = 1$), n_{Se} and n_{Sa} are the nuclear spin statistical weights ($n_{Se}/n_{Sa} = 1:2$ for molecules of G_6 symmetry[22,31]), S_e and S_a are the strengths of the $0a_1$–$0a_1$ and $0e$–$0e$ torsional bands (squared Franck-Condon factors) and n_e/n_a is the population ratio of $0a_1$ and $0e$ torsional states. Under the usual assumption of no collisional population redistribution between $0a_1$ and $0e$ levels during the expansion, the latter ratio is one.

The ground state rotational population, used to calculate the intensities, was described separately for each torsional level. It is given by a two-temperature distribution:[27,32]

$$n_{J,K_a,K_c}(T_1, T_2, w) = e^{-E_{J,K_a,K_c}/kT_1} + we^{-E_{J,K_a,K_c}/kT_2}, \tag{16}$$

where the energies E_{J,K_a,K_c} are pure rotational energies (relative to the lowest $0a_1$ and $0e$ rotational level respectively), and w is the weighting factor for the second temperature. The same weighting factors and rotational temperatures were used to describe the distribution over the $0a_1$ and $0e$ levels.

The final constants are obtained by averaging the results from different measurements of the same spectrum to reduce the errors due to a drift in the relative frequency calibration device. The errors of the constants reported are in most cases determined by the variations within different scans rather than by the statistical errors resulting from the fitting procedure. However, for several parameters the statistical error still dominates.

III. EXPERIMENT

Rotationally resolved fluorescence excitation spectra of 3-MI and 5MI were obtained using a narrow bandwidth UV laser system and a molecular beam apparatus.[33] 3-MI or 5-MI, obtained from Aldrich, was heated to *ca.* 75 °C, seeded in 0.6 bar argon, and expanded through a nozzle with a diameter of about 0.15 mm. The nozzle was kept at a slightly higher temperature than the sample vessel to prevent condensation of the sample in the orifice. The molecular beam was skimmed twice in a differential pumping system and was crossed perpendicularly with a UV laser beam at about 30 cm from the nozzle. The pressure in the detection chamber was below 10^{-6} mbar, assuring collision free conditions. The total undispersed fluorescence was imaged onto a photomultiplier connected to a photon counting system, interfaced with a computer.

UV radiation with a bandwidth of 3 MHz was generated by intracavity frequency doubling in a single frequency ring dye laser, operating on Rhodamine 110 and Rhodamine 6G, respectively, for the 3-MI and 5-MI measurements. By using a 2 mm thick Brewster cut BBO crystal, 0.1 mW of tunable UV radiation was obtained. Light at the fundamental frequency was used for calibration and stabilization purposes. For relative frequency calibration a temperature stabilized Fabry-Perot interferometer was used with a free spectral range of 75 MHz. For absolute frequency calibration the iodine absorption spectrum[34] was recorded simultaneously. The scanning range is typically 2 cm^{-1} at the fundamental frequency.

The spectral resolution of the experimental set-up is determined by the residual Doppler width in the molecular beam and the geometry of the fluorescence collection optics. Although the instrumental Doppler width is not known for specific molecules, it

can be estimated to be ∼16 MHz FWHM from the results of similar experiments on indole, indazole, and benzimidazole, measured previously using this set-up.[27]

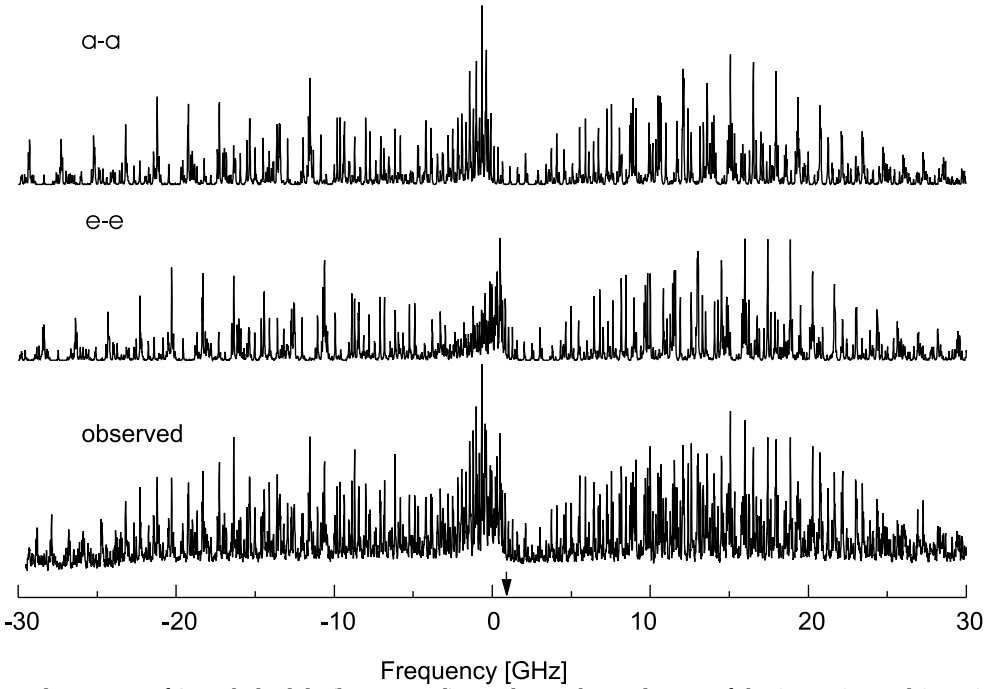

FIG. 4. Experimental spectrum of 3-methylindole (lower panel) together with simulations of the $0a_1 - 0a_1$ and $0e - 0e$ transitions (upper two panels). The $0a_1 - 0a_1$ origin (0 on the scale of the figure) is located at 34874.69(1) cm^{-1}. The origin of the $0e - 0e$ band is indicated by the arrow.

IV. FREQUENCY ANALYSIS

A. 3-methylindole

The observed spectrum of the $S_1 \leftarrow S_0$ origin band of 3-MI is presented in Fig. 4. This spectrum is a composite of the $0a_1$–$0a_1$ and $0e-0e$ spectra, whose simulations are given separately in the upper two panels. The $0e-0e$ spectrum (of which the origin is indicated by an arrow in Fig. 4) is blue shifted with respect to the $0a_1-0a_1$ spectrum, which means that the torsional barrier in the excited state is lower than that in the ground state. The separation between the origins of the $0a_1-0a_1$ and $0e-0e$ spectra, $\Delta\nu_0^{ae}$, was found to be 915 MHz. This separation appears in the spectrum as a spacing between $0a_1-0a_1$ and $0e-0e$ rotational transitions starting from low K_a levels. High K_a levels of the $0e$ states are disturbed by the torsion-rotation interaction, which causes this spacing to no longer be constant.

It was possible to reproduce all observed lines using terms up to $n = 2$ in the Hamiltonian of Eqs. (7) and (12). The analysis started with the simulation of a pure a type spectrum of a rigid asymmetric rotor, using rotational constants calculated from a 3-MI geometry obtained from the attachment of a methyl group to the calculated geometry of indole.[35] By comparison of this simulation with the observed spectrum several $0a_1$–$0a_1$ lines could be assigned. A fit of these lines provided improved rotational constants. Next, we simulated the complete spectrum containing all $0a_1-0a_1$ and $0e-0e$ lines, fixing the distance between the $0a_1$–$0a_1$ and $0e$–$0e$ origins to 915 MHz by adjusting the values of V_3'' and V_3', taken from Ref. 8. Eventually, about 400 $0a_1$–$0a_1$ and 400 $0e-0e$ lines were included in the fit, together with the excited state torsional frequencies of the $2a_1 \leftarrow 0a_1$ band at 188 cm^{-1} and the $2e \leftarrow 0e$ band at 197 cm^{-1}.[8]

Since the spectra did not contain enough information to determine all possible parameters, we made the following assumptions. First, it was assumed that the internal rotation constant of the methyl group does not change upon excitation; *i.e.*, the difference

$F'_\alpha - F''_\alpha$ was fixed to zero. Since the torsion-rotation interaction in the ground state of 3-MI is very small, the calculated spectrum is relatively insensitive to large variations ($\sim 5^\circ$) of the ground state methyl top angle η'' and it turned out to be impossible to fit η'' and $\eta' - \eta''$ simultaneously. We therefore also fixed $\eta' - \eta''$ to zero. The molecular constants obtained from the fit are listed in Table I together with the absolute center frequency of the $0a_1 - 0a_1$ spectrum ν_0^{aa} and several other constants calculated from the fit parameters.

TABLE I. Molecular constants of 3-methylindole. Fitted parameters are given in the upper part, derived parameters in the lower part.

	S_0		S_1		
A'', A'-A''	2603.6(9)		–37.45(3)	MHz	
B'', B'-B''	1268.6(2)		–18.30(2)	MHz	
C'', C'-C''	857.7(1)		–12.40(2)	MHz	
F_α		5.17(3)		cm^{-1}	a
V_3	500(40)		301(1)	cm^{-1}	a
η		50.1(9)		deg	a
θ		±26.3(9)		deg	b
θ_T		±0.7(3)		deg	b
ν_0^{aa}		34874.69(1)		cm^{-1}	
$\Delta\nu_0^{ae}$		914.7(4)		MHz	
ΔE_{ae}	90(40)		1005(40)	MHz	
I_α	3.26(2)		3.26(2)	amuÅ^2	
F	5.23(3)		5.23(3)	cm^{-1}	
$W_{0e}^{(1)}$	$-7(3)\times10^{-4}$		$-77(3)\times10^{-4}$		c
$W_{0a}^{(2)}$	$8(4)\times10^{-4}$		$93(3)\times10^{-4}$		
$W_{0e}^{(2)}$	$-4(2)\times10^{-4}$		$-47(2)\times10^{-4}$		
$FW_{0e}^{(1)}\rho_a$	–1.2(5)		–12.9(6)	MHz	cd
$FW_{0e}^{(1)}\rho_b$	–0.7(3)		–7.5(3)	MHz	cd

[a] $F''_\alpha = F'_\alpha$, $V''_6 = V'_6 = 0$, and $\eta'' = \eta'$ is assumed.
[b] The signs of θ and θ_T cannot be independently determined from the fit. They are, however, coupled: both must either be positive or negative.
[c] $W_{0e}^{(1)}$ is given for $\sigma = +1$. The value for $\sigma = -1$ is given by $-W_{0e}^{(1)}$.
[d] $FW_{0e}^{(2)}\rho_g^2$, $g = a, b$ are < 0.02 MHz for S_0 and < 0.2 MHz for S_1.

Due to the high torsional barriers in both electronic states of 3-MI, the effective rotational constants for the $0a_1$–$0a_1$ and $0e$–$0e$ spectra differ by less than 0.2 MHz from the 'torsion-free' values. This implies that the $0a_1-0a_1$ spectrum is practically that of a rigid asymmetric molecule with the same rotational constants and the perturbations of the $0e$–$0e$ spectrum are mainly determined by the first-order terms in the effective rotational Hamiltonian.

As can be seen from Table I, the torsion induced splittings of the $0e$–$0e$ levels in the ground state ($\sim 2K_a F W_{0e}^{(1)} \rho_a$) reach a value that is comparable to the linewidth only at $K_a > 10$. Since the intensities of these lines are already negligible, it is impossible to obtain the ground state barrier height V_3'' directly from these splittings. V_3'' is determined via the excited state torsional parameters and the separation of the origins of the $0a_1 - 0a_1$ and $0e - 0e$ spectra, $\Delta\nu_0^{ae}$ [Eq. (14)]. This separation is directly determined from the observed spectrum, while V_3' is determined by a combination of the two torsional frequencies included in the fit and the perturbations of the $0e-0e$ lines of the observed spectrum. It follows therefore that the uncertainties of both barrier heights V_3'' and V_3' largely depend on the torsional frequencies, which are accurate to 1 cm^{-1}.

B. 5-methylindole

The spectrum of the $S_1 \leftarrow S_0$ origin band of 5-MI consists, like that of 3-MI, of a $0a_1 - 0a_1$ and a $0e - 0e$ spectrum. Fig. 5 presents the observed spectrum (lower panel) together with simulations of the two separate $0a_1-0a_1$ and $0e-0e$ spectra (upper panels). The $0e-0e$ spectrum is again blue shifted with respect to the $0a_1-0a_1$ spectrum, indicating a lowering of the torsional barrier upon excitation, in this case by a substantially larger amount.

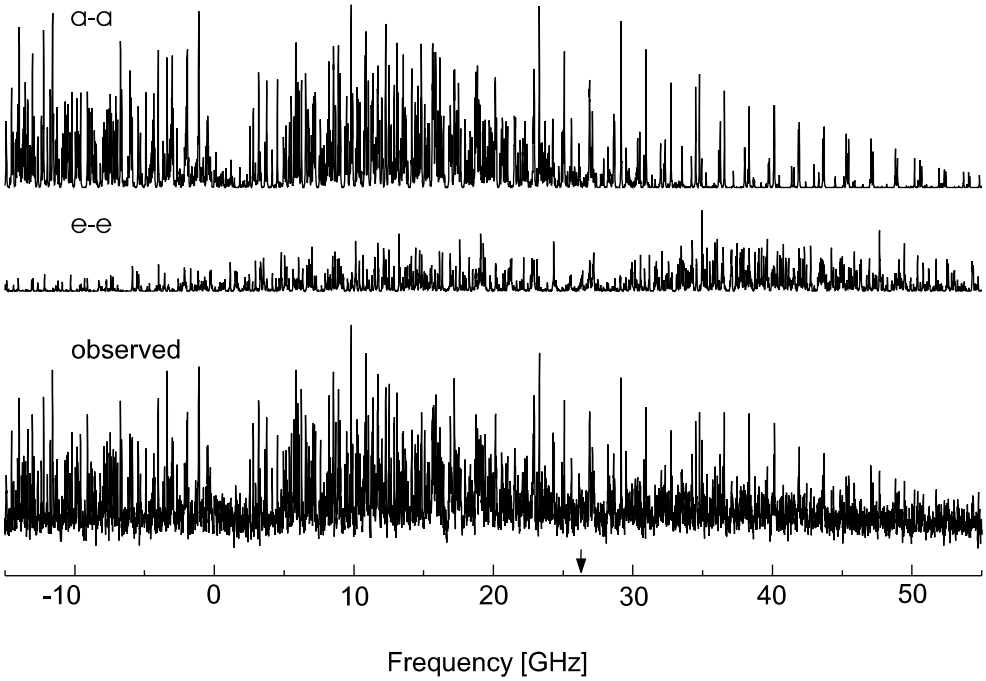

FIG. 5. Experimental spectrum of 5-methylindole (lower panel) together with simulations of the $0a_1 - 0a_1$ and $0e - 0e$ transitions (upper two panels). The $0a_1 - 0a_1$ origin (0 on the scale of the figure) is located at 34355.915(12) cm^{-1}. The origin of the $0e - 0e$ band is indicated by the arrow.

Terms up to $n = 4$ in the effective rotational Hamiltonian [Eqs .(7) and (12)] were necessary to reproduce the observed spectrum. The geometry of 5-MI was again constructed from the combination of a methyl group and an indole frame, which yielded the initial rotational constants. A hybrid asymmetric rotor spectrum was simulated and several $0a_1$–$0a_1$ lines were assigned. A fit of these lines provided the effective rotational constants for the $0a_1$ levels of the ground and the excited state of 5-MI. Assigning the $0e$–$0e$ lines was more troublesome than for 3-MI, because the origin of the $0e$–$0e$ spectrum is more shifted from the $0a_1$–$0a_1$ origin. Furthermore, the overall intensity of the $0e-0e$ spectrum is about three times less than that of the $0a_1-0a_1$ spectrum. The distance between the origins was first crudely estimated and the values of the 3-fold barrier heights V_3'' and V_3', taken from Ref. 7, were slightly adjusted to yield the correct $\Delta\nu_0^{ae}$ value ($\sim$0.9 cm^{-1}). These values enabled us to determine the perturbation coefficients from which we could calculated 'torsion-free' rotational constants for the ground and the excited state. In the next step these constants were used to simulate the composite spectrum of the $0a_1$–$0a_1$ and $0e$–$0e$ bands. Finally about 400 $0a_1$–$0a_1$ and 200 $0e-0e$ transitions were included into the fit. The final parameters are given in Table II.

TABLE II. Molecular constants of 5-methylindole. Fitted parameters are given in the upper part, derived parameters in the lower part.

	S_0		S_1		
A'', A'-A''	3459.9(1)		–132.85(4)	MHz	
B'', B'-B''	1034.06(5)		–0.81(1)	MHz	
C'', C'-C''	800.29(4)		–7.65(1)	MHz	
F_α		5.24(1)		cm^{-1}	[a]
V_3	135(6)		85(1)	cm^{-1}	
V_6	–21(13)		–14(3)	cm^{-1}	
η		–16.9(4)		deg	[b]
θ		53(1)		deg	
θ_T		0.4(2)		deg	
ν_0^{aa}		34355.915(12)		cm^{-1}	
$\Delta\nu_0^{ae}$		26325(2)		MHz	
ΔE_{ae}	18381(12)		44705(14)	MHz	
I_α	3.219(3)		3.219(3)	amuÅ^2	
F	5.348(6)		5.344(6)	cm^{-1}	
$W_{0e}^{(1)}$	–0.1431(3)		–0.3693(6)		[b]
$W_{0a}^{(2)}$	0.1625(3)		0.3745(5)		
$W_{0e}^{(2)}$	–0.0809(2)		–0.1788(2)		
$FW_{0e}^{(1)}\rho_a$	–483.6(3)		–1199.6(4)	MHz	[b]
$FW_{0e}^{(1)}\rho_b$	43.9(7)		113(2)	MHz	[b]
$FW_{0a}^{(2)}\rho_a^2$	11.585(3)		24.667(3)	MHz	
$FW_{0e}^{(2)}\rho_a^2$	–5.764(2)		–11.773(3)	MHz	[c]

[a] F_α and η are assumed to be the same for S_0 and S_1.
[b] $W_{0e}^{(1)}$ is given for $\sigma = +1$. The value for $\sigma = -1$ is given by $-W_{0e}^{(1)}$.
[c] $FW_{0a}^{(2)}\rho_b^2$ and $FW_{0e}^{(2)}\rho_b^2$ are < 0.1 MHz for S_0 and < 0.3 MHz for S_1.

Five excited-state torsional frequencies (39.5, 52, 74.6, 94.4, 155.5 and 203.1 cm^{-1}),[8] and six ground-state torsional frequencies (60.2, 101.3, 122.4, 166.7 228.9, 295.3 cm^{-1}),[7] were included into the fit. Thanks to this large number of torsional transitions also the 6-fold barrier heights V_6'' and V_6' could be determined. Within the errors η'' and η' yielded identical values in the attempt to fit both parameters. Therefore $\eta' - \eta''$ was fixed to zero. Furthermore, it was assumed that $F'_\alpha - F''_\alpha = 0$.

As can be seen from Table II the difference between 'effective' A and 'torsion-free' A constants, determined by $FW^{(2)}_{0a}\rho_a^2$ and $FW^{(2)}_{0e}\rho_a^2$, is quite significant ($\sim$25 MHz for the $0a_1$ states of S_1) and is different for $0a_1-0a_1$ and $0e-0e$ spectra. The difference for the B constants is less than 0.3 MHz.

V. INTENSITY ANALYSIS

With the parameters obtained from the frequency analysis kept fixed, the intensities of the rotational lines can now be analyzed. The results, which are averages of the results from fits of several measurements, are given in Table I and Table II. Both molecules show an ab hybrid spectrum and undergo a reorientation of the inertial axes upon electronic excitation. For 5-MI it was possible to determine the signs of θ and θ_T. Information about the relative signs of the angles θ, θ_T, and η can only be obtained from the intensities. The $0a_1 - 0a_1$ spectrum behaves effectively as an ordinary asymmetric rotor spectrum and it is therefore only sensitive to the relative signs of θ and θ_T, as in indole.[27] The intensities of the $0e - 0e$ lines, however, depend on the relative signs of angles θ, θ_T and η. Therefore, since the sign of η is fixed by the geometry, the signs of θ and θ_T can be determined. For 5-MI this results in a TM angle θ that is $+53^\circ$ and a reorientation angle θ_T that is $+0.4^\circ$. The effect on the intensities of a change of θ and θ_T is demonstrated in Fig. 6. For 3-MI the interference effects are not large enough to affect the intensities appreciably. It is therefore only possible to derive the relative signs of θ ($\theta = \pm 26.3^\circ$) and θ_T ($\theta_T = \pm 0.7^\circ$), yielding the same sign for both angles.

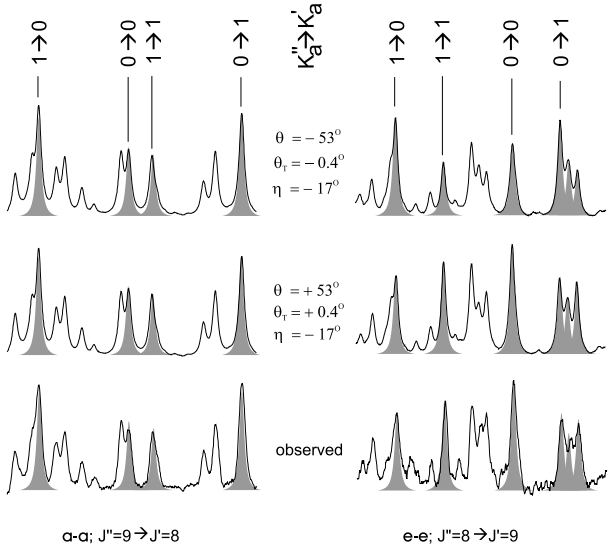

FIG. 6. Parts of the $0a_1 - 0a_1$ and $0e - 0e$ spectrum of 5-methylindole. The lower panels show the observed spectrum. The middle panels show simulations, using positive values for the transition moment and axis reorientation angle. A simultaneous change of sign of θ and θ_T does not affect the line positions but yields different intensities for the $0e - 0e$ transitions, as can be seen from the upper panels.

The intensity ratio I_e/I_a found for 3-MI is approximately unity, in agreement with Eq. (15); the band strength ratio S_e/S_a is predicted to be 1.0, using the constants given in Table I. For 5-MI a value of 0.25 ± 0.10 was found for the intensity ratio, again in agreement with the band strength ratio, which, using the constants given in Table II, is predicted to be 0.304.

A Voigt line-profile was used in the fit of the observed spectrum. For 3-MI it was not possible to fit both the Lorentzian and Gaussian contributions to the linewidth. Therefore, we fixed the Gaussian contribution to 16 MHz, a value determined earlier for this experimental setup.[27] The resulting Lorentzian contribution to the linewidth was found to be 21 ± 3 MHz. Lifetime measurements of 3-MI by Demmer *et al.*[11] and Arnold *et al.*[3] yielded 12.3 ns and 13.8 ± 0.2 ns respectively. These result in Lorentzian contributions to the linewidth of only 12.9 MHz and 11.5 ± 0.2 MHz respectively. A similar line broadening, although less, was also found for indole and indazole.[27] For 5-MI we were able to fit both linewidth parameters, which yielded 17 ± 5 MHz and 10 ± 5 MHz for the Gaussian and the Lorentzian contribution respectively. This latter value corresponds to a lifetime of 15 ± 8 ns.

VI. DISCUSSION

The torsional barriers found for 3-MI are less accurate than those for 5-MI, but all values, where relevant, are in agreement with values found earlier.[7,8] For both molecules the 3-fold barrier lowers by about a factor of 1.6 upon electronic excitation, which accounts for the blue shift of the $0e-0e$ origin with respect to the $0a_1-0a_1$ origin. 3-MI and 5-MI provide a nice example for comparing small and large internal rotation effects. The torsional barrrier heights for 5-MI are about four times lower than those for 3-MI. This leads to larger torsional tunneling splittings (the $0a_1-0e$ distance ΔE_{ae}) for 5-MI, and larger distortions in the rotational spectrum of 5-MI compared to 3-MI. Therefore, fourth-order perturbation theory was necessary to describe the 5-MI spectrum while second-order theory was sufficient to describe the 3-MI spectrum. Despite this, the effects of K_c mixing can clearly be distinguished in the spectrum of 3-MI, as is illustrated in Fig. 3.

The 3-fold barrier heights are related to the electron densities in the molecular frame at the site to which the methyl group is attached. In 3-MI the electron density is distributed asymmetrically around this site, which accounts for the large 3-fold barrier found for 3-MI. The much lower 3-fold and appreciable 6-fold barrier found for 5-MI can be explained by the much more symmetrical electron distribution in the benzene ring. The lowering of the 3-fold barrier upon electronic excitation indicates a shift of the electron distribution in the two molecules towards a more symmetrical distribution around the methyl group site.

Both 3-MI and 5-MI show hybrid type spectra. The 3-MI spectrum is predominantly *a*-type ($|\theta| = 26^\circ$), while that of 5-MI is predominantly *b*-type ($\theta = +53^\circ$). By virtue of the interference term in the intensity formula [Eq. (11)], arising from both axis reorientation and the interaction between internal and overall rotation, it was possible to determine the sign of the transition moment angle of 5-MI. This was found to be in agreement with several semi-empirical and *ab initio* calculations, which yield values between $+35^\circ$ and $+72^\circ$ for the TM angle of indole (for a review see Ref. 36). It also agrees with the conclusion of Philips and Levy, who, after comparing the transition moment angles of tryptamine and indole, concluded that the transition moment angle of indole should be positive.[37] It is also consistent with the measurements of Albinsson *et al.*,[18] who determined the angles θ of indole, 3-MI and 5-MI in polyethylene to be, respectively, $+42^\circ \pm 3^\circ$, $+30^\circ \pm 2^\circ$ and $+58^\circ \pm 2^\circ$. From this we conclude that also for 3-MI θ (and hence θ_T, which is found to have the same sign as θ) should be positive. Assuming that the direction of the TM with respect to the indole frame is the same in 3-MI and 5-MI as it is in indole, the TM angle in 3-MI and 5-MI can be calculated from the TM angle of indole. MP2/6-31G* geometry optimizations[38] were performed on 3-MI and 5-MI to ensure that the structure of the indole frame does not change significantly upon the attachment of a methyl group. This yielded 16° and 49° for the TM angles of 3-MI and 5-MI, respectively. The latter value is in reasonable agreement with the experimental value found for 5-MI, $53^\circ \pm 1^\circ$, implicating that the addition of a methyl group at C-5 only slightly influences the electron density changes in the indole frame upon excitation. For 3-MI however, the calculated value deviates much more from the experimental value, $26.3^\circ \pm 0.9^\circ$, implicating a larger influence of the methyl group.

The axis reorientation angles found for 3-MI and 5-MI (respectively 0.7° and 0.4°) are, as expected, comparable to the value found for indole (0.5°[27]). Geometry calculations on the first excited singlet state were performed by adding the excited state CIS/3-21G and ground state HF/3-21G coordinate differences to the MP2/6-31G* ground state coordinates. The axis reorientation angle can subsequently be calculated using:[39]

$$\tan\theta_T = \frac{\sum_i m_i (a_i' b_i'' - b_i' a_i'')}{\sum_i m_i (a_i' a_i'' + b_i' b_i'')}, \tag{17}$$

where m_i are the atomic masses and a_i', b_i', a_i'', b_i'' are the ground and excited state atomic coordinates, expressed in their inertial axis systems. For 5-MI this yielded a value of 0.4°, in good agreement with the measurements. For 3-MI calculations always converged into the ^1L_a electronic state, which can be explained by the near degeneracy of the predicted ^1L_a and ^1L_b electronic states. No reorientation angle for excitation to the ^1L_b state could therefore be determined.

VII. SUMMARY

The rotationally resolved excitation spectra of the $S_1(^1L_b) \leftarrow S_0$ origin bands of 3-MI and 5-MI have been measured and analyzed. The rotational constants in the ground and electronically excited state have been determined for both molecules. These constants can be used to validate geometry calculations of these molecules. The transition moment angle was also determined from the spectra, consisting of two overlapping transitions between different torsional levels, which originate from the internal rotation of the methyl group. The spectra could be reproduced by describing the interaction between the overall rotation of the molecule and the internal rotation as a perturbation on the rotation. From the frequency analysis the rotational constants, the torsional barrier heights in the ground and electronically excited states, and the angle of the methyl top axis were determined. Intensity analysis of the spectra yielded values for the TM and axis reorientation angles.

ACKNOWLEDGMENTS

Erko Jalviste gratefully acknowledges funding from the Nederlandse Organisatie voor Wetenschappelijk Onderzoek (NWO) and the Estonian Science Foundation (grant n.2270). Ivan Mistrík acknowledges the EPS/SOROS student mobility program for the financial support. This work was made possible by funding from the Dutch Foundation for Fundamental Research on Matter (FOM).

---

[1] H. Lami and N. Glasser, J. Chem. Phys. **84**, 597 (1986).
[2] P. R. Callis, J. Chem. Phys. **95**, 4230 (1991).
[3] S. Arnold and M. Sulkes, J. Phys. Chem. **96**, 4768 (1992), and references therein.
[4] W. J. Hehre, J. A. Pople, and A. J. P. Devaquet, J. Am. Chem. Soc. **98**, 664 (1976).
[5] A. E. Dorigo, D. W. Pratt, and K. N. Houk, J. Am. Chem. Soc. **109**, 6591 (1987).
[6] L. H. Spangler and D. W. Pratt, in Jet Spectroscopy and Molecular Dynamics, ed. by J. M. Hollas and D. Phillips, Blackie Academic and Professional, 1995.
[7] G. A. Bickel, G. W. Leach, D. R. Demmer, J. W. Hager, and S. C. Wallace, J. Chem. Phys. **88**, 1 (1988).
[8] D. M. Sammeth, S. S. Siewert, P. R. Callis, and L. H. Spangler, J. Phys. Chem. **96**, 5771 (1992).
[9] The levels are labeled by their ν value, whereas in Ref. 8 the free rotor label m is used.
[10] A. A. Rehms and P. R. Callis, Chem. Phys. Letters **140**, 83 (1987).
[11] D. R. Demmer, G. W. Leach, and S. C. Wallace, J. Phys. Chem. **98**, 12834 (1994).
[12] E. H. Strickland and C. Billups, Biopolymers **12**, 1989 (1973).
[13] J. R. Cable, J. Chem. Phys. **92**, 1627 (1990).
[14] D. M. Sammeth, S. Yan, L. H. Spangler, and P. R. Callis, J. Phys. Chem. **94**, 7340 (1990).
[15] D. M. Sammeth, S. S. Siewert, L. H. Spangler, and P. R. Callis, Chem. Phys. Lett. **193**, 532 (1992).
[16] B. J. Fender, D. M. Sammeth, and P. R. Callis, Chem. Phys. Letters **239**, 31 (1995).
[17] B. J. Fender and P. R. Callis, Chem. Phys. Letters **262**, 343 (1996).
[18] B. Albinsson and B. Nordén, J. Phys. Chem. **96**, 6204 (1992).
[19] X. Q. Tan, W. A. Majewski, D. F. Plusquellic, and D. W. Pratt, J. Chem. Phys. **94**, 7721 (1991).
[20] G. Berden, W. L. Meerts, M. Schmitt, and K. Kleinermanns, J. Chem. Phys. **104**, 972 (1996).
[21] S. J. Humphrey and D. W. Pratt, J. Chem. Phys. **106**, 908 (1997).
[22] C. C. Lin and J. D. Swalen, Rev. Modern. Phys. **31**, 841 (1959).
[23] J. T. Hougen, I. Kleiner, and M. Godefroid, J. Mol. Spectrosc. **163**, 559 (1994).
[24] W. Gordy and R. L. Cook, *Microwave Molecular Spectra*, 3rd ed. (John Wiley & Sons, New York, 1984).
[25] D. R. Herschbach, J. Chem. Phys. **31**, 91 (1959).
[26] The use of a different basis set, in which the symmetric top basis functions are related to the a-axis (the I representation) and the matrix elements of both J_a and J_b are real, (a convention also used by Hougen *et al.* in Ref. 23), will slightly alter the coefficients of the matrix elements. The methyl top axis is in the ab plane ($\rho_c = 0$). Two matrix elements were found to differ from those given in Ref. 25: $\langle K|(\rho_a J_a + \rho_b J_b)^4|K\rangle = \rho_a^4 K^4 + \frac{1}{2}\rho_a^2\rho_b^2[(P^2-K^2)(6K^2+1) - 4K^2] + \frac{1}{8}\rho_b^4[3(P^2-K^2)^2 - 2(P^2-K^2) + 3K^2]$ and $\langle K|(\rho_a J_a + \rho_b J_b)^4|K \pm 1\rangle = \rho_a^3(2K \pm 1)[K^2 + (K \pm 1)^2] + \frac{1}{2}\rho_a\rho_b^2(2K \pm 1)\{3[P^2 - K(K \pm 1)] - 4\}$.
[27] G. Berden, E. Jalviste, and W. L. Meerts, J. Chem. Phys. **103**, 9596 (1995).
[28] A. A. Held, B. B. Champagne, and D. W. Pratt, J. Chem. Phys. **95**, 8732 (1991).
[29] It should be kept in mind that the angle of the transition dipole moment θ is given with respect to the a''-axis, as well as the methyl top axis in the ground state, η'', which is embedded in ρ_a and ρ_b, but the corresponding angle in the excited state, η', is still defined with respect to the a'-axis.
[30] D. F. Plusquellic and D. W. Pratt, J. Chem. Phys. **97**, 8970 (1992).
[31] L. H. Spangler and D. W. Pratt, J. Chem. Phys. **84**, 4789 (1986).
[32] Y. R. Wu and D. H. Levy, J. Chem. Phys. **91**, 5278 (1989).
[33] W. A. Majewski and W. L. Meerts, J. Mol. Spectrosc. **104**, 271 (1984).
[34] S. Gerstenkorn and P. Luc, *Atlas du spectroscopie d'absorption de la molecule d'iode* (CNRS, Paris, 1978), S. Gerstenkorn and P. Luc, Rev. Phys. Appl. **14**, 791 (1979).
[35] L. S. Slater and P. R. Callis, J. Phys. Chem. **99**, 8572 (1995).
[36] P. R. Callis, Meth. in Enzymology **278**, 113 (1997).
[37] L. A. Philips and D. H. Levy, J. Phys. Chem. **90**, 4921 (1986).
[38] Gaussian 94, Revision D.2, M. J. Frisch, G. W. Trucks, H. B. Schlegel, P. M. W. Gill, B. G. Johnson, M. A. Robb, J. R. Cheeseman, T. Keith, G. A. Petersson, J. A. Montgomery, K. Raghavachari, M. A. Al-Laham, V. G. Zakrzewski, J. V. Ortiz, J. B. Foresman, J. Cioslowski, B. B. Stefanov, A. Nanayakkara, M. Challacombe, C. Y. Peng, P. W. Ayala, W. Chen, M. W. Wong, J. L. Andres, E. S. Replogle, R. Gomperts,

R. L. Martin, D. J. Fox, J. S. Binkley, D. J. Defrees, J. Baker, J. P. Stewart, M. Head-Gordon, C. Gonzalez, and J. A. Pople, Gaussian, Inc., Pittsburgh PA, 1995.
[39] J. T. Hougen and J. K. G. Watson, Can. J. Phys. **43**, 298 (1965).